

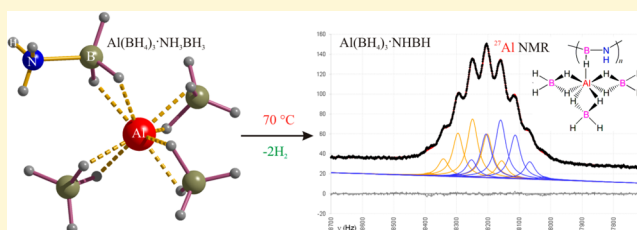
# Mild Dehydrogenation of Ammonia Borane Complexed with Aluminum Borohydride

Iurii Dovgaliuk, Cécile S. Le Duff, Koen Robeyns, Michel Devillers, and Yaroslav Filinchuk\*

Institute of Condensed Matter and Nanosciences, Université catholique de Louvain, 1348 Louvain-la-Neuve, Belgium

**S** Supporting Information

**ABSTRACT:** Ammonia borane is a promising hydrogen store. However, its dehydrogenation is stepwise, nonreversible, and accompanied by formation of undesirable byproducts. We report on a new  $\text{Al}(\text{BH}_4)_3 \cdot \text{NH}_3\text{BH}_3$  complex containing 17.7 wt % hydrogen, which undergoes a two-step thermal decomposition below 100 °C. The combination of volumetric, gravimetric, crystallographic, and nuclear magnetic resonance studies shows that both in the solid state and in toluene solutions, the Al-coordinated  $\text{NH}_3\text{BH}_3$  already releases two  $\text{H}_2$  molecules per Al at 70 °C. Contrary to that of the pristine ammonia borane, this process is endothermic, suggesting a possibility for direct rehydrogenation. The dehydrogenation of  $\text{Al}(\text{BH}_4)_3 \cdot \text{NH}_3\text{BH}_3$  contrasts with the complete destruction of alkali and alkaline earth metal borohydride complexes with ammonia borane in the first decomposition step. Other Al-based Lewis acids, less challenging with respect to the stability and safety than  $\text{Al}(\text{BH}_4)_3$ , may be good agents for supporting the reversible dehydrogenation of  $\text{NH}_3\text{BH}_3$  under mild conditions.



## INTRODUCTION

In recent years, metal borohydrides  $\text{M}(\text{BH}_4)_n$ <sup>1,2</sup> and  $\text{M}-\text{B}-\text{N}-\text{H}$  systems<sup>3,4</sup> of metal amidoboranes (MABs), amine metal borohydrides (AMBs), and complexes with ammonia borane  $\text{NH}_3\text{BH}_3$  (AB) have been among the most attractive materials for potential solid-state hydrogen storage as they exceed by far the year 2017 system targets of 5.5 wt % hydrogen and 40 g/L gravimetric density set by the U.S. Department of Energy.<sup>5</sup> Several metal borohydrides  $\text{M}(\text{BH}_4)_n$  ( $n = 1$ ,  $\text{M} = \text{Li}^+$  or  $\text{Na}^+$ ;<sup>6,7</sup>  $n = 2$ ,  $\text{M} = \text{Be}^{2+}$ ,  $\text{Mg}^{2+}$ , or  $\text{Ca}^{2+}$ ;<sup>8–10</sup>  $n = 3$ ,  $\text{M} = \text{Al}^{3+}$  or  $\text{Ti}^{3+11,12}$ ) have been studied as potential hydrogen storage media. However, the hydrogen desorption temperatures for alkali and most alkaline earth metal borohydrides are far from the range of 60–120 °C useful for hydrogen fuel cells:<sup>13</sup> indeed, desorption temperatures of ~470 °C for  $\text{LiBH}_4$  and 290–500 °C for  $\text{Mg}(\text{BH}_4)_2$  and  $\text{Al}(\text{BH}_4)_3$  with  $\text{Be}(\text{BH}_4)_2$  make them unpractical. The high stability of borohydrides can be decreased using formation of bimetallic borohydrides. Their stability decreases with increasing Pauling electronegativity ( $\chi_p$ ) of the complex-forming cation.<sup>14,15</sup> The most unstable metal borohydride complexes contain highly electronegative  $\text{Al}^{3+}$ ,  $\text{Zn}^{2+}$ , and  $\text{Cd}^{2+}$  ( $\chi_p$  values of 1.61, 1.65, and 1.69, respectively), which create weaker B–H bonds, together with alkali metal cations ( $0.79 \leq \chi_p \leq 0.98$ ). In particular, the series of bimetallic borohydrides of  $\text{Al}_3\text{Li}_4(\text{BH}_4)_{13}$ ,  $\text{NaAl}(\text{BH}_4)_x\text{Cl}_{4-x}$ ,  $\text{KAl}(\text{BH}_4)_4$ ,<sup>16–18</sup>  $\text{LiZn}_2(\text{BH}_4)_5$ ,  $\text{NaZn}_2(\text{BH}_4)_5$ ,  $\text{NaZn}(\text{BH}_4)_3$ , and  $\text{KZn}(\text{BH}_4)_3$ <sup>19,20</sup> as well as  $\text{KCa}(\text{BH}_4)_3$  and  $\text{K}_2\text{Cd}(\text{BH}_4)_4$ <sup>21</sup> decompose at rather low temperatures. However, they evolve toxic diborane  $\text{B}_2\text{H}_6$  during decomposition, which contaminates the fuel cells and decreases the reversibility of these potential materials.

Another group of materials with competitive hydrogen storage properties consists of metal borohydride complexes with ammonia and ammonia borane,  $\text{NH}_3\text{BH}_3$ . The presence of  $\text{N}-\text{H}^{\delta+} \cdots \text{H}^{\delta-}-\text{B}$  dihydrogen bonds in these compounds considerably decreases the dehydrogenation temperatures, to the range of 60–250 °C. Several amine metal borohydrides (AMBs) are considered promising hydrogen storage materials:  $\text{LiBH}_4 \cdot \text{NH}_3$ ,<sup>22,23</sup>  $\text{M}(\text{BH}_4)_2 \cdot 2\text{NH}_3$  ( $\text{M} = \text{Mg}^{2+}$ ,  $\text{Ca}^{2+}$ , or  $\text{Zn}^{2+}$ ),<sup>24–26</sup>  $\text{Ti}(\text{BH}_4)_3 \cdot 3\text{NH}_3$ ,<sup>27</sup>  $\text{Al}(\text{BH}_4)_3 \cdot n\text{NH}_3$ ,<sup>28,29</sup>  $\text{LiMg}(\text{BH}_4)_3 \cdot 2\text{NH}_3$ ,<sup>30,31</sup>  $\text{Li}_2\text{Ti}(\text{BH}_4)_5 \cdot 5\text{NH}_3$ , and  $\text{Li}_2\text{Al}(\text{BH}_4)_5 \cdot 6\text{NH}_3$ .<sup>27,32</sup> The hydrogen decomposition properties of AMBs are affected both by the nature of the metal cation and by the number of coordinated ammonia molecules per cation. It was reported that  $\text{LiBH}_4 \cdot \text{NH}_3$  and  $\text{Ca}(\text{BH}_4)_2 \cdot 2\text{NH}_3$  mainly release ammonia rather than hydrogen under dynamic flow,<sup>33,34</sup> however, cobalt-catalyzed thermolysis of  $\text{LiBH}_4 \cdot \text{NH}_3$  releases 17.8 wt %  $\text{H}_2$ .<sup>34</sup> The other representatives,  $\text{Mg}(\text{BH}_4)_2 \cdot 2\text{NH}_3$  and  $\text{Al}(\text{BH}_4)_3 \cdot 6\text{NH}_3$ , produce only traces of ammonia,<sup>24,28</sup> while  $\text{Zn}(\text{BH}_4)_2 \cdot 2\text{NH}_3$ ,  $\text{Ti}(\text{BH}_4)_3 \cdot 3\text{NH}_3$ , and  $\text{Al}(\text{BH}_4)_3 \cdot 4\text{NH}_3$ - $\text{LiBH}_4$  composite, bimetallic  $\text{LiMg}(\text{BH}_4)_3 \cdot 2\text{NH}_3$ ,  $\text{Li}_2\text{Ti}(\text{BH}_4)_5 \cdot 5\text{NH}_3$ , and  $\text{Li}_2\text{Al}(\text{BH}_4)_5 \cdot 6\text{NH}_3$  release high-purity hydrogen.<sup>24,27,28</sup> The detailed electronic structure of  $\text{M}(\text{BH}_4)_2 \cdot 2\text{NH}_3$  ( $\text{M} = \text{Mg}^{2+}$ ,  $\text{Ca}^{2+}$ , or  $\text{Zn}^{2+}$ ) reveals a highly ionic character of  $\text{Ca}^{2+}$  in  $\text{Ca}(\text{BH}_4)_2 \cdot 2\text{NH}_3$  and partial covalence of  $\text{Mg}-\text{NH}_3$  and  $\text{Zn}-\text{NH}_3$ , which prevents the release of  $\text{NH}_3$  from the latter complexes.<sup>35</sup>

Received: September 30, 2014

Revised: December 13, 2014

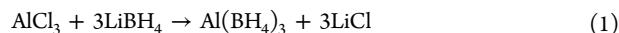
Published: January 15, 2015

Despite the high hydrogen content of ammonia borane (~19.6%) and acceptable stability upon transportation and storage,  $\text{NH}_3\text{BH}_3$  undergoes stepwise decomposition with 6.5% hydrogen released below 112 °C and 14.5% near 200 °C, all accompanied by undesirable borazine and aminoborane  $\text{NH}_2\text{BH}_2$ .<sup>36,37</sup> A considerable improvement is achieved by forming metal salts of ammonia borane. This improves the decomposition temperature to ~90 °C for Li- or  $\text{NaNH}_2\text{BH}_3$ ,<sup>38</sup> giving way to a large family of materials. Ammonia borane metal-containing derivatives (MABs)  $\text{M}(\text{NH}_2\text{BH}_3)_n$  ( $n = 1$ ,  $\text{M} = \text{Li}^+$  or  $\text{Na}^+$ ;  $n = 2$ ,  $\text{M} = \text{Ca}^{2+}$  or  $\text{Mg}^{2+}$ ),<sup>38–41</sup> including bimetallic  $\text{NaLi}(\text{NH}_2\text{BH}_3)_2$  and  $\text{Na}_2\text{Mg}(\text{NH}_2\text{BH}_3)_4$  and mixed-anion  $\text{Li}_2(\text{NH}_2\text{BH}_3)(\text{BH}_4)/\text{LiNH}_2\text{BH}_3$ , were obtained in recent years.<sup>42–44</sup> All the listed MABs release hydrogen as well as toxic ammonia and traces of  $\text{NH}_2\text{BH}_2$ . For the mixed MAB–AB complex  $\text{LiNH}_2\text{BH}_3 \cdot \text{NH}_3\text{BH}_3$ , the hydrogen release was reported to be occur to 14.0 wt % in a stepwise manner at 80 and 140 °C, and neither borazine nor aminoborane was detected.<sup>45</sup> Metal borohydride–ammonia borane complexes  $\text{M}(\text{BH}_4)_n(\text{NH}_3\text{BH}_3)_m$  ( $n = 1$ ,  $m = 1$  or  $2$  for  $\text{M} = \text{Li}^+$ ;  $n = m = 2$  for  $\text{M} = \text{Ca}^{2+}$  or  $\text{Mg}^{2+}$ ) showed more facile hydrogen desorption with less ammonia evolution compared to the case for pure ammonia borane and MABs.<sup>46–49</sup> Further improvements in the properties of these complexes were achieved by combining some AMBs with ammonia borane, such as  $\text{Li}_2\text{Al}(\text{BH}_4)_3(\text{NH}_3\text{BH}_3)_3 \cdot 6\text{NH}_3$  and  $\text{Mg}(\text{BH}_4)_2 \cdot 2\text{NH}_3 \cdot \text{NH}_3\text{BH}_3$ , where high-purity hydrogen was released.<sup>50,48</sup>

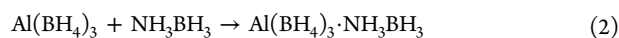
Compounds in Al–B–N–H systems are among the best in terms of hydrogen storage properties. However, the number of components involved goes increasingly high, leaving little (if any) chance for their reversibility. Here we report a new  $\text{Al}(\text{BH}_4)_3 \cdot \text{NH}_3\text{BH}_3$  complex with 17.7 wt % hydrogen, combining only two hydrogen rich molecules:  $\text{Al}(\text{BH}_4)_3$  and  $\text{NH}_3\text{BH}_3$ . Remarkably, the complexation transforms aluminum borohydride into a stable solid, which undergoes a two-step thermal decomposition at temperatures below 100 °C. We report on the synthesis, crystal structures, and Raman spectroscopic studies of the complex, as well as thermal analysis,  $^{11}\text{B}$  and  $^{27}\text{Al}$  nuclear magnetic resonance (NMR) spectroscopy, and volumetric studies of its decomposition and reversibility.

## EXPERIMENTAL SECTION

**Synthesis. Caution!**  $\text{Al}(\text{BH}_4)_3$  is a highly pyrophoric liquid that explodes on contact with air. All manipulations were conducted in a nitrogen-filled drybox. The reactions were performed using commercially available reagents:  $\text{AlCl}_3$  and  $\text{NH}_3\text{BH}_3$  (both from Sigma-Aldrich at  $\geq 95\%$  purity) and  $\text{LiBH}_4$  ( $\geq 96\%$  purity, Boss chemical industry Co.). The  $\text{Al}(\text{BH}_4)_3 \cdot \text{NH}_3\text{BH}_3$  complex was obtained by a two-step synthesis. The first step involves formation of  $\text{Al}(\text{BH}_4)_3$  by a metathesis reaction:



We used the same procedure described in our previous work,<sup>16</sup> which is a modification of an earlier one.<sup>51</sup> The final product is obtained by the following addition reaction:



For that purpose, 1 mL of freshly obtained liquid  $\text{Al}(\text{BH}_4)_3$  is injected via syringe into a bottle with 70 mg of  $\text{NH}_3\text{BH}_3$  powder. The bottle is kept sealed for 72 h until large white crystals form (Figure S1 of the Supporting Information). The excess of liquid  $\text{Al}(\text{BH}_4)_3$  was pumped off during 30 s. The obtained crystals self-ignite when they come into contact with moisture and air.

**X-ray Single-Crystal Analysis.** The complex reveals two polymorphs. The crystals of  $\alpha\text{-Al}(\text{BH}_4)_3 \cdot \text{NH}_3\text{BH}_3$  were selected in the argon-filled glovebox and then measured at 100 K under a nitrogen flow (Oxford Cryosystems). For better completeness, two crystals were measured independently using a PILATUS 2M pixel detector and  $\lambda = 0.82103$  Å synchrotron X-ray radiation at the SNBL beamline, ESRF (Grenoble, France). The recorded data were indexed in monoclinic space group  $P2_1/c$  with  $a = 7.8585(2)$  Å,  $b = 6.8647(1)$  Å,  $c = 15.7136(8)$  Å, and  $\beta = 96.429(4)^\circ$  and integrated by CrysAlisPro;<sup>52</sup> the implemented absorption correction was applied. The data from the two crystals were integrated separately and scaled (not merged) in XPREP (Bruker) prior to structure solution and refinement.

Data for  $\beta\text{-Al}(\text{BH}_4)_3 \cdot \text{NH}_3\text{BH}_3$  were collected on a MAR345 image plate detector (Mo  $K\alpha$  radiation, Zr filter). The crystals of  $\beta\text{-Al}(\text{BH}_4)_3 \cdot \text{NH}_3\text{BH}_3$  were loaded into inert grease in an argon-filled glovebox and then measured at 295 K under a nitrogen flow (Oxford Cryosystems). The recorded data were indexed in a monoclinic cell and integrated with CrysAlisPro, and the absorption correction was applied.<sup>52</sup> The structure was determined in space group  $Cc$  with  $a = 10.8196(8)$  Å,  $b = 7.2809(4)$  Å,  $c = 11.3260(9)$  Å, and  $\beta = 107.69(1)$ , with a pseudoinversion symmetry for 83% of the structure, as determined by ADDSYM in Platon.

All single-crystal structures were solved by direct methods and refined by a full matrix least-squares method on  $F^2$  using SHELXL2014.<sup>53</sup>

**X-ray Powder Diffraction.** For variable-temperature *in situ* powder X-ray diffraction, the crystals of  $\alpha$ - and  $\beta\text{-Al}(\text{BH}_4)_3 \cdot \text{NH}_3\text{BH}_3$  were ground in an agate mortar inside the argon-filled glovebox and the powders were introduced into 0.7 mm glass capillaries that were sealed with vacuum grease. The capillaries were steadily heated from 20 to 100 °C with a nitrogen blower (Oxford Cryosystems) with heating rates of 1 and 0.2 °C/min. The two-dimensional data images obtained at SNBL were azimuthally integrated with Fit2D using  $\text{LaB}_6$  as a calibrant.<sup>54</sup> The Rietveld method was used for the phase analysis and refinement with Fullprof Suite.<sup>55</sup>

**NMR Spectroscopy.** NMR spectra were acquired in toluene- $d_8$  on a Bruker Avance DRX500 spectrometer operating at 500.1 for  $^1\text{H}$  (160.5 MHz for  $^{11}\text{B}$  and 130.3 MHz for  $^{27}\text{Al}$ ). Chemical shifts are reported with reference to  $\text{SiMe}_4$  (TMS) for  $^1\text{H}$ ,  $\text{BF}_3 \cdot \text{OEt}_2$  for  $^{11}\text{B}$ , and 1.1 M  $\text{Al}(\text{NO}_3)_3$  in  $\text{D}_2\text{O}$  for  $^{27}\text{Al}$ . Spectra were measured on solutions of  $\alpha\text{-Al}(\text{BH}_4)_3 \cdot \text{NH}_3\text{BH}_3$  crystals, as well as on the starting products  $\text{Al}(\text{BH}_4)_3$  and  $\text{NH}_3\text{BH}_3$  dissolved in toluene- $d_8$  for reference. After dissolving the crystals of  $\alpha\text{-Al}(\text{BH}_4)_3 \cdot \text{NH}_3\text{BH}_3$ , we measured the evolution of spectra with time: fresh, after 2 h, and after 18 h. Other samples studied by NMR were aged at room temperature for 2 months and heated under argon up to 70 °C and up to 100–110 °C in sealed glass bottles using a mineral oil bath for 40 and 60 min, respectively. The residues were dissolved in toluene- $d_8$  and measured at room temperature.

The deconvolution processing for  $^{27}\text{Al}$  NMR spectra included one level of zero filling, exponential multiplication of the free induction decay with a line broadening (lb) factor of 1 Hz, Fourier transform, and zero-order phase correction; no correction of the initial decay, no first-order phase correction, and no baseline correction were applied. The region between 8700 Hz (66.76 ppm) and 7700 Hz (59.09 ppm) was submitted to deconvolution analyses using a homemade program developed in Excel. The  $^{27}\text{Al}$  NMR signal was described as a first-order multiplet, constraining intensity ratios according to Pascal's triangle and imposing a Lorentzian line shape and identical line width for all of the components. A second-order polynomial (three adjustable parameters) accounted for the local baseline.

NMR data of the compounds recognized in the presented spectra.  $\text{B}_2\text{H}_6$ :  $^1\text{H}$  NMR  $\delta$  3.89 (q,  $^1J_{\text{B,H}} = 132$  Hz, external hydrogens),  $-0.8$  ( $^1J_{\text{B,H}} = 44$  Hz, bridging hydrogens);  $^{11}\text{B}$  NMR  $\delta$  17.6–17.8 (tt,  $^1J_{\text{B,H}} = 132$  Hz);  $^{11}\text{B}\{^1\text{H}\}$  NMR  $\delta$  17.6 (s). Presumably  $\text{Al}(\text{BH}_4)_3 \cdot \text{NH}_3\text{BH}_3$ :  $^{11}\text{B}$  NMR  $\delta$   $-21.8$  (quadruplet,  $^1J_{\text{B,H}} = 92$  Hz,  $\text{BH}_3$ ),  $-33.8$  (quint,  $^1J_{\text{B,H}} = 88$  Hz,  $\text{BH}_4^-$ );  $^{11}\text{B}\{^1\text{H}\}$  NMR  $\delta$   $-21.9$  (s,  $\text{BH}_3$ ),  $-34.1$  (s,  $\text{BH}_4^-$ );  $^{27}\text{Al}$  NMR  $\delta$  60.3 (s, broad);  $^{27}\text{Al}\{^1\text{H}\}$  NMR  $\delta$  60.3 (s). Decomposition product, presumably  $\text{Al}(\text{BH}_4)_3 \cdot \text{NHBH}$  or its oligomer:

$^{11}\text{B}$  NMR  $\delta$   $-34.4$  (quint,  $^1J_{\text{B,H}} = 86$  Hz,  $\text{BH}_4^-$ );  $^{11}\text{B}\{^1\text{H}\}$  NMR  $\delta$   $-34.4$  (s,  $\text{BH}_4^-$ );  $^{27}\text{Al}$  NMR  $\delta$   $63.0$  [nonuplet (doublet of heptuplets),  $J_{\text{doublet}} = 89.4$  Hz,  $J_{\text{heptuplet}} = 46.4$  Hz,  $\text{BH}_4^-$ , and  $^1J_{\text{Al,H}}$ ];  $^{27}\text{Al}\{^1\text{H}\}$  NMR  $\delta$   $63.0$  (s).

**Raman Spectroscopy.** Raman spectra with 1064 nm excitation were recorded from 4000 to  $100\text{ cm}^{-1}$  with a Bruker RFS 100/s FT-Raman spectrometer ( $I = 200$  mW) at room temperature using a diode-pumped, air-cooled Nd:YAG laser for excitation. The powder sample was placed in a 0.7 mm glass capillary under argon and sealed with vacuum grease. Variable-temperature Raman spectroscopy was performed using the same spectrometer and temperature control chamber under an argon flow. The spectra were recorded in a stepwise manner every  $5^\circ\text{C}$  from 30 to  $125^\circ\text{C}$ .

**TGA, DSC, and MS Analyses.** TGA and DSC analyses were performed on powder samples after preliminary X-ray powder diffraction analysis. The data were collected with TGA/SDTA 851 Mettler and DSC 821 Mettler devices with heating rates of 1 and  $5^\circ\text{C}/\text{min}$  from 25 to  $200^\circ\text{C}$ . The samples for the TGA and DSC analyses were loaded in the argon-filled glovebox into crucibles with caps and sealed into aluminum pans, respectively. The experiments were conducted under a nitrogen flow of 10 mL/min to prevent hydrolysis or oxidation.

Mass spectrometry (MS) analysis of the residual gas was performed using a Hiden Analytical HPR-20 QMS sampling system. The samples (each approximately 2 mg) were loaded into an  $\text{Al}_2\text{O}_3$  crucible and heated from room temperature to  $70^\circ\text{C}$ , fixing this temperature for 2 h ( $1^\circ\text{C}/\text{min}$  for both) in an argon flow of 20 mL/min. The decomposition up to  $200^\circ\text{C}$  was measured by a ThermoStar GSD 301T spectrometer coupled with a simultaneous TGA/DTA 851 Mettler device. The released gases were analyzed for hydrogen, ammonia, diborane, and borazine in both experiments.

**Volumetric Study.** Volumetric analysis was performed using a Hiden Isochema IMI-SHP analyzer. Four decomposition experiments with the  $\text{Al}(\text{BH}_4)_3\cdot\text{NH}_3\text{BH}_3$  complex were conducted with 50–60 mg of sample, under a 5 bar back-pressure of hydrogen/helium, from 30 to  $70^\circ\text{C}$  and from 30 to  $100^\circ\text{C}$  at a heating rate of  $1^\circ\text{C}/\text{min}$ . The gas release was calculated from the calibrated volumes of the system, excluding the volume of the glass wool ( $2.06\text{ g}/\text{cm}^3$ ). Rehydrogenation of the samples decomposed at 70 and  $100^\circ\text{C}$  was conducted at  $\sim 150$  bar of hydrogen, by heating them to 70 and  $100^\circ\text{C}$  and cooling them to  $30^\circ\text{C}$  at a rate of  $0.1^\circ\text{C}/\text{min}$ .

## RESULTS AND DISCUSSION

$\text{Al}(\text{BH}_4)_3\cdot\text{NH}_3\text{BH}_3$  can be obtained from commercially available chemicals,  $\text{AlCl}_3$ ,  $\text{LiBH}_4$ , and  $\text{NH}_3\text{BH}_3$ , in two steps. The synthesis requires an inert atmosphere as the intermediate  $\text{Al}(\text{BH}_4)_3$  is highly pyrophoric.<sup>16</sup> The reaction of  $\text{Al}(\text{BH}_4)_3$  with powder  $\text{NH}_3\text{BH}_3$  at room temperature gives white crystals (see Figure S1 of the Supporting Information). The reaction was allowed to proceed on average for 3 days. Ball milling is expected to dramatically accelerate the reaction on a large scale; however, one should avoid extended vacuum pumping of the excess  $\text{Al}(\text{BH}_4)_3$ , as it decreases the yield of the product.

The detailed characterization of the complex is presented below. It aimed first to identify its different crystal forms coexisting under ambient conditions, second to improve our understanding of its complex dehydrogenation, and third to determine the nature of the Al-based intermediate species.

**Crystal Structure of the Complex.** We have characterized two polymorphs of  $\text{Al}(\text{BH}_4)_3\cdot\text{NH}_3\text{BH}_3$ : the low-temperature  $\alpha$ -phase and the high-temperature  $\beta$ -phase.  $\alpha$ - $\text{Al}(\text{BH}_4)_3\cdot\text{NH}_3\text{BH}_3$  is observed only in freshly synthesized samples, while it slowly transforms at room temperature into the  $\beta$ -phase. In both structures, aluminum atoms coordinate three  $\text{BH}_4^-$  anions and one  $\text{NH}_3\text{BH}_3$  molecule, forming a mononuclear  $\text{Al}(\text{BH}_4)_3\cdot\text{NH}_3\text{BH}_3$  heteroleptic complex, like the one shown in Figure 1. Weak dihydrogen bonds between  $\text{BH}_4^-$  and  $-\text{NH}_3$  groups

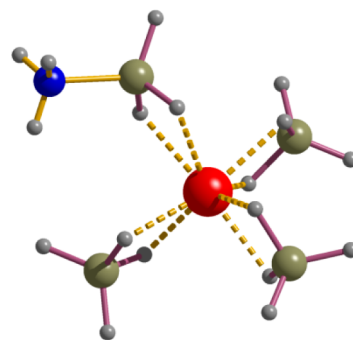


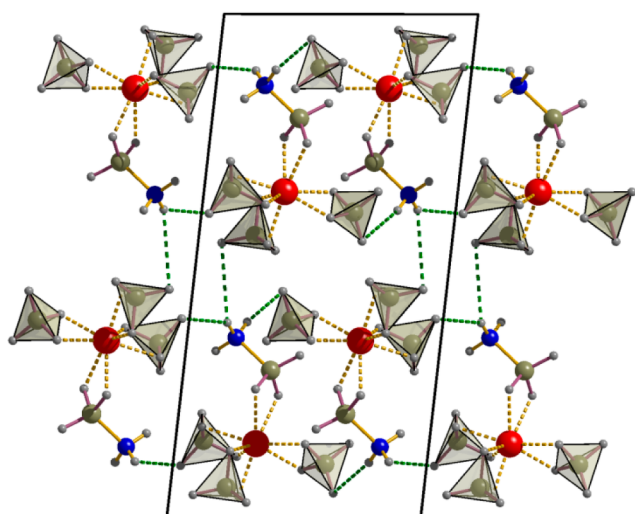
**Figure 1.** Isolated  $\text{Al}(\text{BH}_4)_3\cdot\text{NH}_3\text{BH}_3$  complex, in which the  $\text{Al}^{3+}$  cation coordinates three  $\text{BH}_4^-$  anions and one  $\text{NH}_3\text{BH}_3$  molecule.

associate the complexes into a three-dimensional structure.  $\text{N}-\text{H}^{\sigma^+}\cdots\text{H}^{\sigma^-}-\text{B}$  bonds are often bifurcated on the  $\text{N}-\text{H}$  side; thus, the  $\text{H}\cdots\text{H}$  distances are rather long, exceeding 2.6 Å, while  $\text{N}-\text{H}^{\sigma^+}\cdots\text{H}^{\sigma^-}$  angles are not very close to  $180^\circ$  (see Table S6 of the Supporting Information).

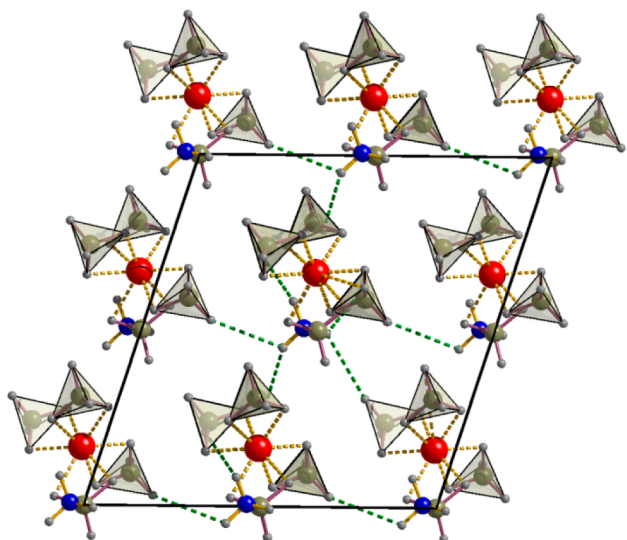
The  $\text{Al}^{3+}$  cation is linked via  $\text{BH}_2$  edges to three  $\text{BH}_4^-$  anions and to one ammonia borane molecule. With respect to B atoms, Al adopts a distorted tetrahedral coordination, and the  $\text{AlH}_8$  polyhedron has the shape of a snub disphenoid, like that of Mg in  $\text{Mg}(\text{BH}_4)_2$  structures.<sup>56,57</sup> This contrasts with planar trigonal  $\text{AlB}_3$ /trigonal prismatic  $\text{AlH}_6$  coordination in both known polymorphs of  $\text{Al}(\text{BH}_4)_3$ .<sup>58,59</sup> The Al–B distances with  $\text{BH}_4^-$  ions are in the narrow range of 2.21–2.23 Å and are slightly longer than 2.10–2.15 Å as determined by gas electron diffraction and in the solid  $\alpha,\beta$ - $\text{Al}(\text{BH}_4)_3$ .<sup>58,59</sup> It is nearly identical to the 2.22–2.26 Å Al–B distances in  $\text{K}[\text{Al}(\text{BH}_4)_4]$  and  $[\text{Ph}_3\text{MeP}][\text{Al}(\text{BH}_4)_4]$ , where the  $\text{Al}^{3+}$  cation is also coordinated to eight hydrogen atoms.<sup>16,60</sup> The interatomic Al–B distances involving ammonia borane's  $\text{BH}_3$  group are slightly longer (2.31 Å) than the distances to the  $\text{BH}_4^-$  anions. They are still much shorter than metal–boron distances in other borohydride– $\text{NH}_3\text{BH}_3$  complexes, namely, 2.63–2.92 Å in  $(\text{LiBH}_4)_2\cdot\text{NH}_3\text{BH}_3$ ,  $\text{LiBH}_4\cdot\text{NH}_3\text{BH}_3$ , and  $\text{Ca}(\text{BH}_4)_2\cdot 2\text{NH}_3\text{BH}_3$ .<sup>46,47</sup> The Al–H bond distances vary accordingly: they range from 1.65(8)–1.81(1) Å where  $\text{BH}_4^-$  is involved, similar to those in Al-based complex hydrides,<sup>22,60</sup> to 1.86(1)–1.96(8) Å where the  $\text{BH}_3$  group is involved. The latter are much shorter than the 2.44 and 2.50 Å Al–H bond distances in  $\text{Ca}(\text{BH}_4)_2\cdot(\text{NH}_3\text{BH}_3)_2$  and the 2.08–2.32 Å distances in  $(\text{LiBH}_4)_2\cdot\text{NH}_3\text{BH}_3$ .

**Relative Stability of the Polymorphs.** The phase analysis by X-ray powder diffraction was performed prior to further characterization of the complex by other techniques. Both  $\alpha$ - and  $\beta$ - $\text{Al}(\text{BH}_4)_3\cdot\text{NH}_3\text{BH}_3$  can be obtained as single phases using the synthesis procedures described above (Figure 2). Figure S2 of the Supporting Information shows Rietveld refinement profiles for single-phase samples of the  $\alpha$ - and  $\beta$ -polymorphs.  $\alpha$ - $\text{Al}(\text{BH}_4)_3\cdot\text{NH}_3\text{BH}_3$  was found as a single phase only in freshly prepared samples. Within a few days at room temperature, we find a mixture of the two phases. The crystals of the  $\beta$ -phase cooled to 100 K did not turn into the  $\alpha$ -phase; thus, the  $\alpha$  to  $\beta$  transition is irreversible or at least slow.

Variable-temperature *in situ* powder X-ray diffraction of both polymorphs at a heating rate of  $1^\circ\text{C}/\text{min}$  (Figure 3) reveals that  $\alpha$ - $\text{Al}(\text{BH}_4)_3\cdot\text{NH}_3\text{BH}_3$  undergoes a first-order phase transition to  $\beta$ - $\text{Al}(\text{BH}_4)_3\cdot\text{NH}_3\text{BH}_3$  at  $\sim 62^\circ\text{C}$ ; the latter is melting and presumably decomposing at  $\sim 71^\circ\text{C}$ . The heating of the single-phase sample of the  $\beta$ -phase with a 5-fold lower



a)



b)

**Figure 2.** Association of molecular  $\text{Al}(\text{BH}_4)_3 \cdot \text{NH}_3\text{BH}_3$  complexes by dihydrogen bonds in (a) the  $\alpha$ -phase and (b) the  $\beta$ -phase.

rate of  $0.2\text{ }^\circ\text{C}/\text{min}$  reveals melting at the lower temperature of  $52\text{ }^\circ\text{C}$  (see Figure S3 of the Supporting Information), thus confirming the simultaneous decomposition.

**Raman Spectroscopy.** The Raman spectrum of  $\beta\text{-Al}(\text{BH}_4)_3 \cdot \text{NH}_3\text{BH}_3$  is shown in Figure 4. Several stretching B–H modes can be recognized in the  $2080\text{--}2600\text{ cm}^{-1}$  range, similar to the vibrational modes of  $[\text{Al}(\text{BH}_4)_4]^-$  and  $\text{Al}(\text{BH}_4)_3$ , where  $\text{BH}_4^-$  is coordinated to  $\text{Al}^{3+}$  in a bidentate manner.<sup>22,61</sup> Three intense peaks at  $2441$ ,  $2496$ , and  $2530\text{ cm}^{-1}$  probably belong to the outward B–H (terminal) stretching modes from different  $\text{BH}_4$  and  $\text{BH}_3$  groups; the peaks from  $2040$  to  $2300\text{ cm}^{-1}$  correspond to inward B–H (bridging with Al) stretching modes. The vibrations between  $950$  and  $1650\text{ cm}^{-1}$  can be attributed to B–H bending, and the peaks near  $490\text{ cm}^{-1}$  likely correspond to an Al–B stretching band, as observed for  $[\text{Al}(\text{BH}_4)_4]^-$  anion and for  $\text{Al}(\text{BH}_4)_3$ .<sup>22,61,62</sup> The N–H stretching region is represented by two intense peaks at  $3240$  and  $3299\text{ cm}^{-1}$  that are slightly shifted to lower frequencies with respect to the symmetric ( $3250\text{ cm}^{-1}$ ) and antisymmetric ( $3316\text{ cm}^{-1}$ ) stretches in  $\text{NH}_3\text{BH}_3$ .<sup>63</sup> Literature reports the B–

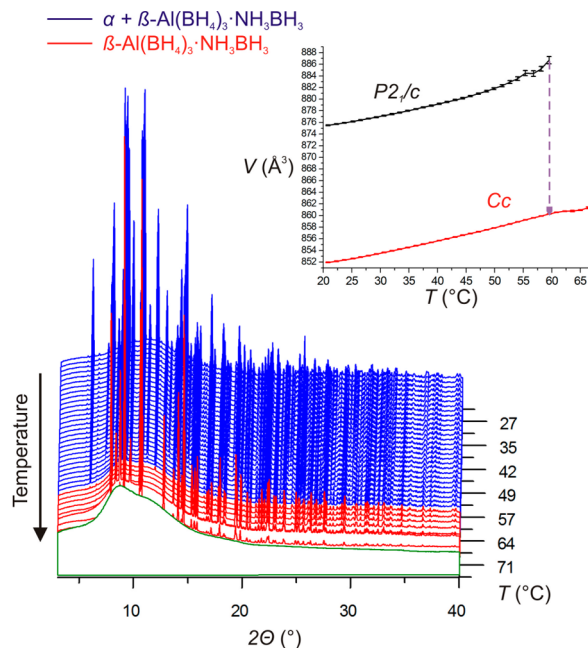


**Figure 3.** Variable-temperature *in situ* synchrotron powder X-ray diffraction of  $\alpha$ - and  $\beta\text{-Al}(\text{BH}_4)_3 \cdot \text{NH}_3\text{BH}_3$  ( $\lambda = 0.821693\text{ \AA}$  from SNBL). The unit cell volume as a function of temperature is shown in the inset.

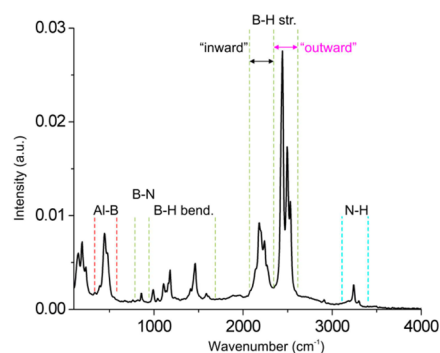
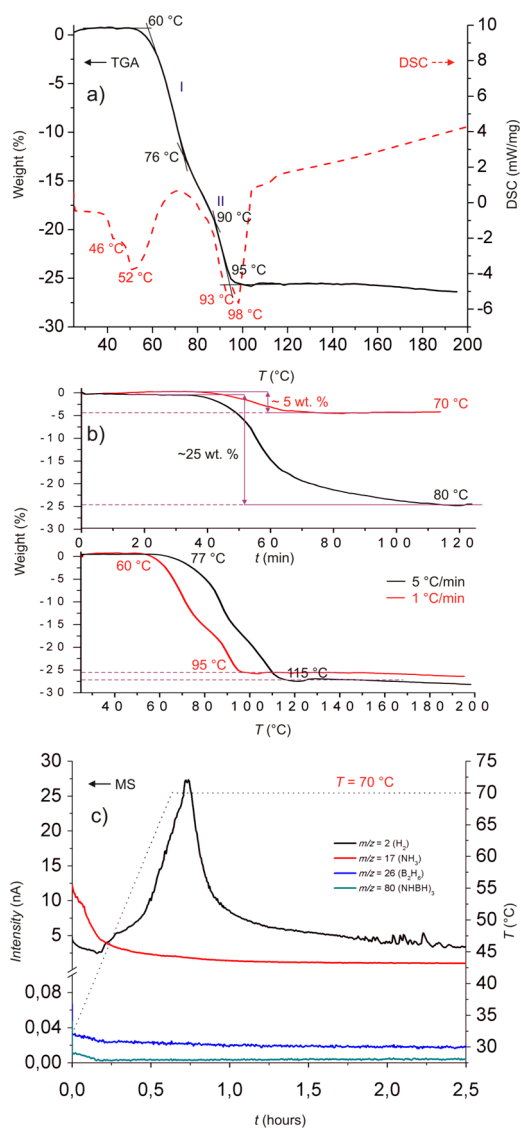


**Figure 4.** Raman spectrum of  $\beta\text{-Al}(\text{BH}_4)_3 \cdot \text{NH}_3\text{BH}_3$ .

N vibrations around  $800\text{ cm}^{-1}$ , and we can surmise that the vibration at  $858\text{ cm}^{-1}$  belongs to the B–N stretch in the coordinated  $\text{NH}_3\text{BH}_3$ .<sup>63</sup>

**Thermal Analysis: Two Decomposition Steps.** Several thermal effects are observed when the samples are heated from  $25$  to  $200\text{ }^\circ\text{C}$  (Figure 5a). The first endothermic ( $\sim 39\text{ kJ/mol}$ ) peak near  $46\text{--}52\text{ }^\circ\text{C}$  (DSC) corresponds to the melting/decomposition of  $\beta\text{-Al}(\text{BH}_4)_3 \cdot \text{NH}_3\text{BH}_3$ . The next endothermic ( $\sim 65\text{ kJ/mol}$ ) peak near  $93\text{ }^\circ\text{C}$  is assigned to the second decomposition step. TGA also displays two decomposition steps: the first starts at  $\sim 60\text{ }^\circ\text{C}$  and finishes at  $\sim 80\text{ }^\circ\text{C}$ , and the second is centered around  $90\text{ }^\circ\text{C}$ . The bottom part of Figure 5b shows that the higher heating rate increases the decomposition temperature from  $\sim 60\text{ }^\circ\text{C}$  for  $1\text{ }^\circ\text{C}/\text{min}$  to  $\sim 77\text{ }^\circ\text{C}$  for  $5\text{ }^\circ\text{C}/\text{min}$ . This behavior is similar to that of ammonia borane, which showed different decomposition reaction pathways depending on the heating rate.<sup>36,37</sup>

We performed additional experiments aiming to separate the two decomposition steps, holding samples at fixed temperatures of  $70$  and  $80\text{ }^\circ\text{C}$ . Remarkably, the mass loss asymptotically reached very different values of  $5$  and  $25\text{ wt } \%$ , respectively (see



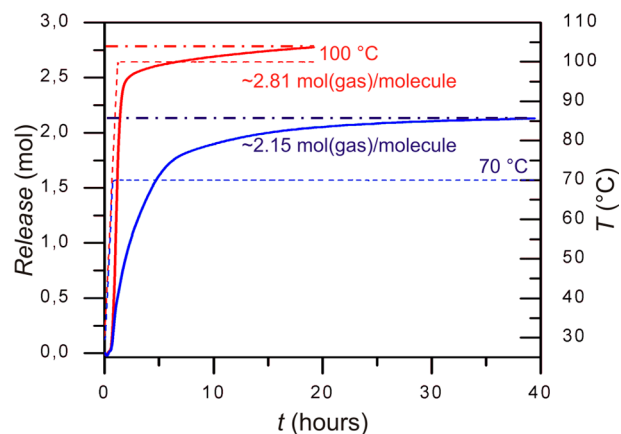
**Figure 5.** Thermal analysis of the  $\text{Al}(\text{BH}_4)_3 \cdot \text{NH}_3\text{BH}_3$  complex: (a) overlap of the TGA and DSC data collected at a rate of  $1^\circ\text{C}/\text{min}$  and (b) weight loss as a function of time, at constant temperatures of  $70^\circ\text{C}$  and  $80^\circ\text{C}$  (top graph), and as a function of heating rate (bottom). (c) MS curves of evolving gases measured in the temperature range of  $30$ – $70^\circ\text{C}$ . The signals of ammonia, diborane, and borazane are close to zero level, which confirms the high purity of hydrogen release at  $70^\circ\text{C}$ .

Figure 5b). The decomposition step at  $70^\circ\text{C}$  with a  $\sim 5$  wt % loss looks very interesting, as it suggests that potentially pure hydrogen is released from the sample (see the Volumetric Study for more details). The decomposition of the other borohydride–ammonia borane complexes,  $\text{M}(\text{BH}_4)_n(\text{NH}_3\text{BH}_3)_m$  ( $n = 1, m = 1$  or  $2$  for  $\text{M} = \text{Li}^+$ ;  $n = m = 2$  for  $\text{M} = \text{Ca}^{2+}$  or  $\text{Mg}^{2+}$ ), yields significant amounts of ammonia, diborane, and borazine besides hydrogen on the first decomposition step.<sup>46–49</sup> While these compounds undergo complete decomposition involving both borohydride and ammonia borane moieties, the thermal analysis of the title complex suggests the release of hydrogen from ammonia borane in the first step, followed by a diborane release (theoretical 27 wt % loss) in the second step. The volumetric and mass spectrometry studies help to verify this hypothesis.

The MS determination of the released gases was made in the same manner as TGA: the first decomposition step is characterized isothermally at  $70^\circ\text{C}$  and the complete decomposition at temperatures above  $100^\circ\text{C}$ . Remarkably, desorption at  $70^\circ\text{C}$  showed exclusively the release of hydrogen, while the possible impurities of ammonia, diborane, and borazane were not detected (see Figure 5c). Further heating provokes release of diborane, which was detected around the start of the second decomposition step at  $85^\circ\text{C}$  (see Figure S4 of the Supporting Information). Variable-temperature *in situ* Raman spectroscopy also confirmed decomposition of the complex around  $75^\circ\text{C}$  (see Figure S5 of the Supporting Information). Unfortunately, the detailed characterization of the decomposition products of the first and second steps was not possible from Raman spectra. Visually, the residue of the fully decomposed (at  $150^\circ\text{C}$ ) samples resembles foamed polymer-like products.

**Volumetric Study of the Decomposition and a Reversibility Test.** Taking into account the information from TGA and DSC analysis, we performed two volumetric measurements at different temperatures:  $70^\circ\text{C}$ , which corresponds to the first decomposition step, and  $100^\circ\text{C}$ , which relates to the second decomposition step.

Samples were steadily heated at a rate of  $1^\circ\text{C}/\text{min}$ , as in the TGA experiment. Decomposition at  $70^\circ\text{C}$  produces  $\sim 1.15$  mmol of gas from  $0.54$  mmol of the starting complex (Figure 6), i.e.,  $2.15$  mol of gas per formula unit (f.u.). To verify this



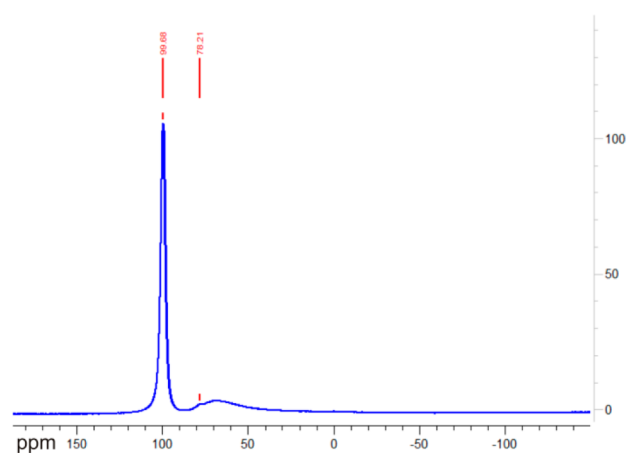
**Figure 6.** Volumetric analysis of  $\text{Al}(\text{BH}_4)_3 \cdot \text{NH}_3\text{BH}_3$  decomposition at  $70^\circ\text{C}$  with  $0.54$  mmol of the complex and at  $100^\circ\text{C}$  with  $0.58$  mmol of the complex, at a heating rate of  $1^\circ\text{C}/\text{min}$ .

result, two additional volumetric experiments were conducted for the first step of the decomposition in He and  $\text{H}_2$  backpressure at  $70^\circ\text{C}$ , yielding  $1.93$  and  $2.10$  mol of gas per f.u. The second decomposition step at  $100^\circ\text{C}$  shows the release of  $\sim 2.81$  mmol of gas per f.u. Using the TGA data, we infer that the first decomposition step gives  $\sim 2$  mol of hydrogen per  $\text{Al}(\text{BH}_4)_3 \cdot \text{NH}_3\text{BH}_3$  unit ( $\sim 5$  wt % mass loss) and the second step gives almost 1 mol of diborane (close to  $\sim 25$  wt % mass loss).

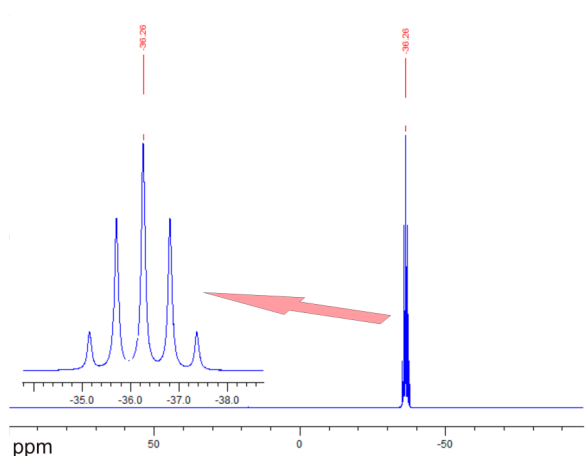
Our attempts to rehydrogenate, at  $150$  bar, the samples decomposed at  $70$  and  $100^\circ\text{C}$  were not successful: the  $\text{H}_2$  pressure returns exactly to the same value after the very slow cooling (see Figure S6 of the Supporting Information).

**NMR Spectroscopy Study of  $\text{Al}(\text{BH}_4)_3 \cdot \text{NH}_3\text{BH}_3$  and Its Decomposition.**  $^1\text{H}$ ,  $^{11}\text{B}$ , and  $^{27}\text{Al}$  NMR spectra were recorded on  $\text{Al}(\text{BH}_4)_3$  prior to being used in the synthesis of

$\text{Al}(\text{BH}_4)_3 \cdot \text{NH}_3\text{BH}_3$  and were found to be in good agreement with the literature.<sup>64</sup> The interpretation of the  $^1\text{H}$  NMR spectra being difficult because of the presence of very broad signals around 0.5 ppm, we focused our attention on the interpretation of  $^{11}\text{B}$  and  $^{27}\text{Al}$  NMR spectra. The main  $^{11}\text{B}$  peak for  $\text{Al}(\text{BH}_4)_3$  is found at  $-36.3$  ppm with a negligible amount of diborane, because of the slow  $\text{Al}(\text{BH}_4)_3$  degradation, present at 17.8 ppm (not even visible in Figure 7b). The main  $^{27}\text{Al}$  peak for



a)



b)

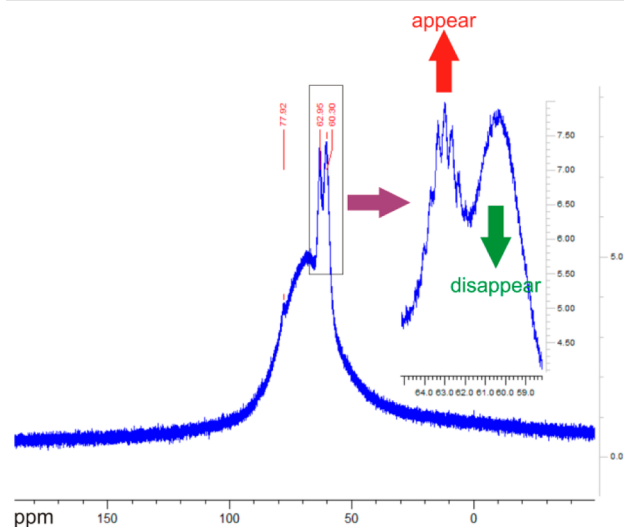
**Figure 7.** (a)  $^{27}\text{Al}$  NMR and (b)  $^{11}\text{B}$  NMR spectra of  $\text{Al}(\text{BH}_4)_3$  in toluene- $d_8$ .

$\text{Al}(\text{BH}_4)_3$  is at 99.7 ppm, and an unknown impurity observed at 78.2 ppm (Figure 7a,b). Broad signals in the spectra originate from the solid Al-containing material in the probe, and from the  $^{11}\text{B}$  in the borosilicate NMR tubes, as proven by blank measurements, and can be removed by using a backward linear prediction during data processing.

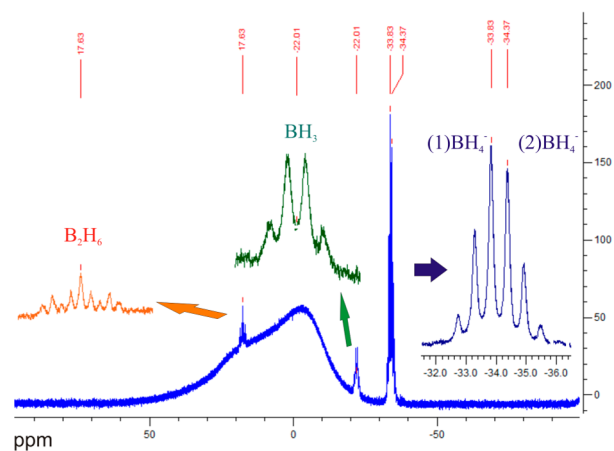
Samples of  $\text{Al}(\text{BH}_4)_3 \cdot \text{NH}_3\text{BH}_3$  stored in a glovebox at 25–30 °C over 2 weeks turned into a viscous mass, prompting us to study by NMR spectroscopy the decomposition products obtained at different temperatures. To observe the changes in  $\text{Al}(\text{BH}_4)_3 \cdot \text{NH}_3\text{BH}_3$ , we performed experiments on (1) a freshly dissolved sample in toluene- $d_8$ , (2) the same sample in solution kept at room temperature for 2 and 18 h, and (3) samples heated to 70 and 100 °C, as in Volumetric Study, and then

dissolved in toluene- $d_8$ . Complete data are shown in Figures S8–S18 of the Supporting Information.

$\text{Al}(\text{BH}_4)_3 \cdot \text{NH}_3\text{BH}_3$  does not decompose into  $\text{Al}(\text{BH}_4)_3$ , as no signal at 99.7 ppm in the  $^{27}\text{Al}$  NMR spectrum appears; instead, we observe a signal at 60.3 ppm that is not present after 18 h. In the  $^{11}\text{B}$  NMR spectrum (Figure 10b), we observe a sextuplet, consisting of two overlapped quintets at  $-33.8$  and  $-34.4$  ppm, and a quadruplet at  $-21.9$  ppm (Figure 8b and



a)



b)

**Figure 8.** (a)  $^{27}\text{Al}$  NMR and (b)  $^{11}\text{B}$  NMR spectra of freshly dissolved  $\text{Al}(\text{BH}_4)_3 \cdot \text{NH}_3\text{BH}_3$  in toluene- $d_8$ .

Figures S9–S12 of the Supporting Information). The presence of a small amount of diborane  $\text{B}_2\text{H}_6$  was observed as a triplet of triplets at 17.5 ppm in the  $^{11}\text{B}$  NMR spectrum.<sup>65</sup> It is likely the result of partial decomposition of  $\text{Al}(\text{BH}_4)_3 \cdot \text{NH}_3\text{BH}_3$  into  $\text{B}_2\text{H}_6$ , as for instance via a reaction



There is no diborane forming up to 70 °C in the absence of the solvent (see the MS data in Figure 5). However, the intensity of the diborane peak increases with time in the toluene solution.

In contrast to the broad signal of the starting compound at 60.3 ppm that disappears over time, the intensity of a nonseptet

at 63.0 ppm increases in the  $^{27}\text{Al}$  NMR spectrum (Figures 8a and 9a). In the  $^{11}\text{B}$  NMR spectrum, a quintet at  $-34.4$  ppm,

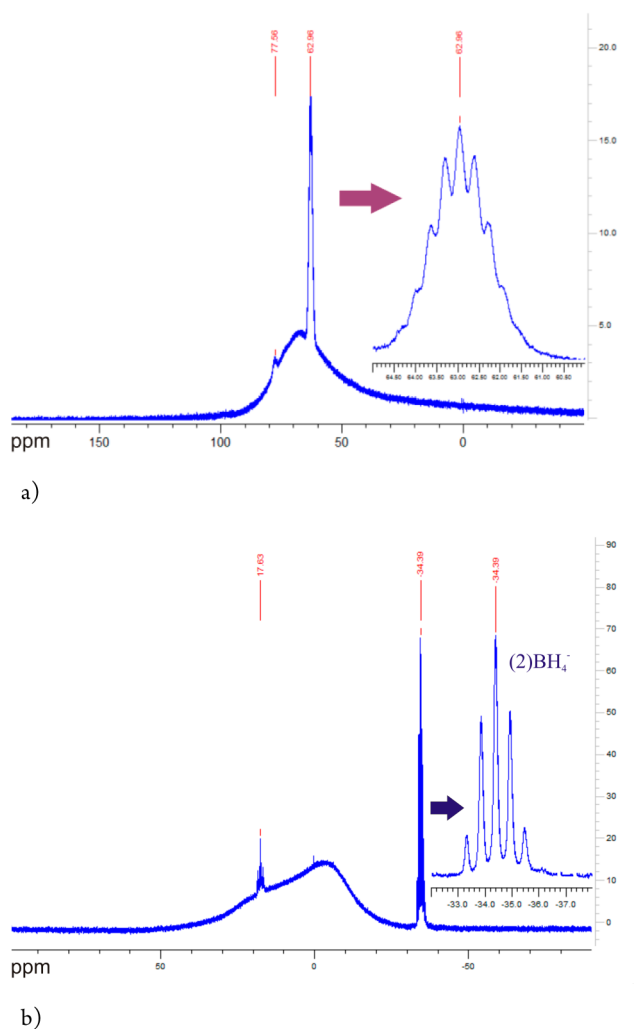


**Figure 9.** (a)  $^{27}\text{Al}$  NMR and (b)  $^{11}\text{B}$  NMR spectra of  $\text{Al}(\text{BH}_4)_3 \cdot \text{NH}_3\text{BH}_3$  dissolved in toluene- $d_8$  after 18 h.

corresponding to  $\text{BH}_4^-$  anion, increasingly dominates the spectrum over the disappearing signal at  $-33.8$  ppm present at 2 and 18 h (Figures 8b and 9b).

In the sample that decomposed at  $\sim 70^\circ\text{C}$ , the same main NMR signals, as in the 18 h-aged sample spectrum, were observed at 63 and  $-34.5$  ppm in the  $^{27}\text{Al}$  and  $^{11}\text{B}$  NMR spectra, respectively (compare Figures 9 and 10). The intensities of the several other minor signals at 82.0, 77.6, and 74.4 ppm changed in the  $^{27}\text{Al}$  spectrum. After  $100^\circ\text{C}$ , we observe (Figure S18 of the Supporting Information) only a single  $^{27}\text{Al}$  NMR signal at 81.9 ppm, which probably has the same nature as that at 82.0 ppm after heating to  $70^\circ\text{C}$  (Figure 10a).

$^{11}\text{B}$  NMR signals at  $-35.0$  ppm are present in all the samples as well as an unknown signal in the  $^{27}\text{Al}$  spectrum and are suspected to belong to  $\text{AlB}_x\text{H}_y$  products, as well as the  $^{11}\text{B}$  signals at  $-36.0$  ppm with  $^{27}\text{Al}$  at 81.9 and 82.0 ppm. They can be the result of reaction of  $\text{B}_2\text{H}_6$  with starting compound or/and forming products previously described for  $\text{Al}(\text{BH}_4)_3$  with  $\text{B}_2\text{H}_6$ , giving the  $\text{AlB}_4\text{H}_{11}$  at  $100^\circ\text{C}$ .<sup>65</sup> The assignment of the remaining weak  $^{11}\text{B}$  signals is not certain, but they likely belong

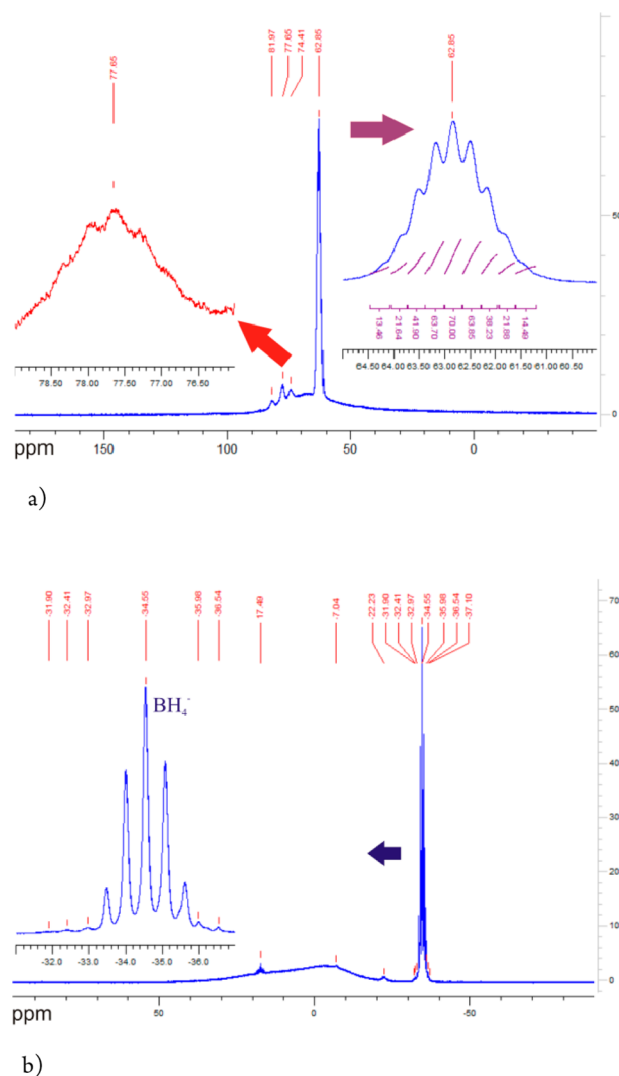


**Figure 10.** (a)  $^{27}\text{Al}$  NMR and (b)  $^{11}\text{B}$  NMR spectra of  $\text{Al}(\text{BH}_4)_3 \cdot \text{NH}_3\text{BH}_3$  heated to  $\sim 70^\circ\text{C}$  and dissolved in toluene- $d_8$ .

to polyhydroboranes. The presence of compounds such as DADB  $[\text{BH}_2(\text{NH}_3)_2]\text{BH}_4$  is excluded because no characteristic  $\text{BH}_2$  signal at approximately  $-15$  ppm on the  $^{11}\text{B}$  spectrum was detected in our experiment.<sup>66</sup>

Notably, the fresh  $\text{Al}(\text{BH}_4)_3 \cdot \text{NH}_3\text{BH}_3$  sample kept in a toluene- $d_8$  solution at room temperature, the sample aged in the inert atmosphere at ambient temperature and then dissolved in toluene- $d_8$  (Figure S19 of the Supporting Information), and the sample heated to  $70^\circ\text{C}$  and then dissolved in toluene- $d_8$  all give the same spectral features. No insoluble products were formed upon their dissolution in toluene. Therefore, it is likely the same decomposition pathway is followed in toluene solutions and in the absence of any solvent. This means we can interpret by NMR the decomposition intermediate obtained in TGA/DSC and volumetric experiments, responsible for the release of 2 mol of  $\text{H}_2$ . Its fingerprint is the nonuplet at 63.0 ppm in the  $^{27}\text{Al}$  NMR spectrum, with an intensity distribution of 14:22:40:64:70:64:40:22:14. With proton decoupling, this nonuplet at 63.0 ppm becomes a singlet (Figures S12a,b and S15a,b), implying the splitting of this peak into nine lines is indeed caused by protons coupled to aluminum. The experimental signal exhibits nine maxima or shoulders, but as

one can see in Figure 11a, it is not properly described by a first-order nonuplet (relative intensity ratios of

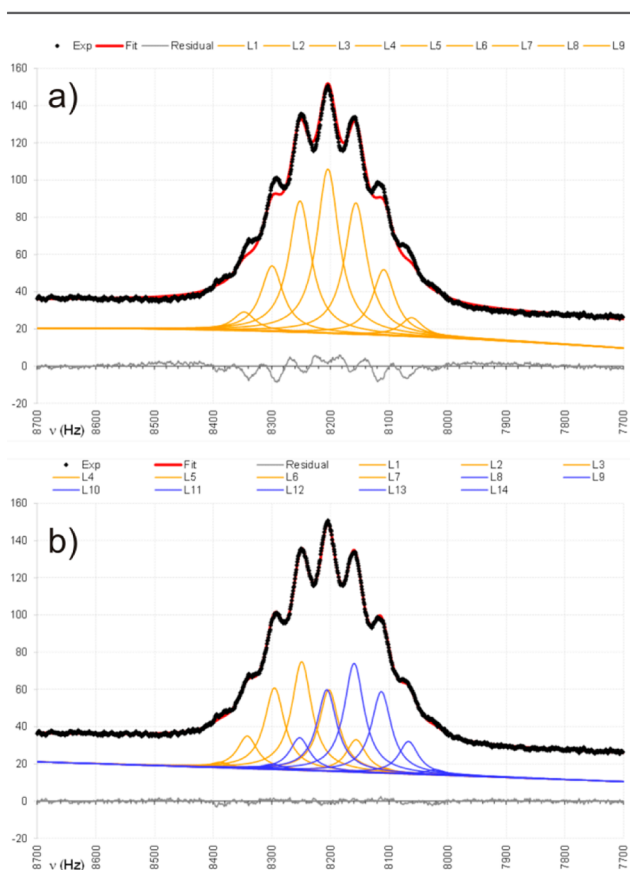
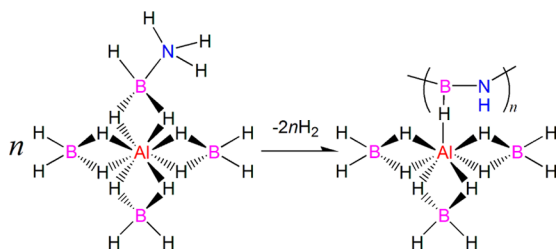


**Figure 11.** Best fit of (a) a first-order nonuplet and (b) a first-order doublet of heptuplets to the  $^{27}\text{Al}$  NMR signal observed at 63.0 ppm.

1:8:28:56:70:56:28:8:1; four adjustable parameters being chemical shift, line width, overall intensity, and one scalar coupling constant). In contrast, considering a doublet of heptuplets as a model yields excellent agreement (Figure 11b; relative intensity ratios of  $\{1:6:15:20:15:6:1\}:\{1:6:15:20:15:6:1\}$ ; five adjustable parameters, including the overall intensity). The relevant best-fit parameters are as follows:  $\delta = 62.954$  ppm,  $\Delta\nu_{1/2} = 40.0$  Hz (full line width at half-height corrected for lb), and scalar coupling constants  $J_{\text{doublet}} = 89.4$  Hz,  $J_{\text{heptuplet}} = 46.4$  Hz. Our observed  $J$  value of 46.4 Hz is similar to that reported for  $^1J_{\text{Al,H}}$  of 44 Hz in  $\text{Al}(\text{BH}_4)_3$ .<sup>67</sup>

**Decomposition Intermediate.** The NMR study shows that the first step of the decomposition of  $\text{Al}(\text{BH}_4)_3 \cdot \text{NH}_3\text{BH}_3$  yields the product in which an Al ion is bound to three borohydride anions with edges and further bound to one hydrogen, most likely a part of an “HN-HB” molecule or its oligomers, as shown here:



This evidence ties in very well with the results of our volumetric/TGA data suggesting the loss of two  $\text{H}_2$  molecules. The  $6\text{H} + 1\text{H}$  coordination of Al in the decomposition intermediate of  $\text{Al}(\text{BH}_4)_3 \cdot \text{NH}_3\text{BH}_3$  is the first evidenced by the deconvolution analysis of the  $^{27}\text{Al}$  NMR spectrum. The molecular structure of the other aluminum borohydride complexes had been previously assigned on the basis of the supposed reaction equilibria in solutions and the known solid-state structures.<sup>60,68</sup> In all cases, the  $\text{BH}_4$  anions are coordinated via the  $\text{BH}_2$  edges. Broad singlets at 49.5 ppm in the spectra of  $[\text{Ph}_3\text{MeP}][\text{Al}(\text{BH}_4)_4]$  and  $[(\text{Ph}_3\text{P})_2\text{N}][\text{Al}(\text{BH}_4)_4]$  in  $\text{CD}_2\text{Cl}_2$  correspond to 8 equiv of H around Al,<sup>60</sup> and that at 99.7 ppm in the spectrum of  $\text{Al}(\text{BH}_4)_3$  corresponds to 6 equiv of H around Al; both are significantly different from the 63.0 ppm shift we observed. The complex with the closest chemical shift is  $[\text{AlH}(\text{BH}_4)_2]_n$  with a signal at 64.7 ppm: it contains 4H from the  $\text{BH}_4$  groups and 2H bridging Al atoms.<sup>64</sup>

## CONCLUSIONS

The thermal decomposition of the new complex,  $\text{Al}(\text{BH}_4)_3 \cdot \text{NH}_3\text{BH}_3$ , showed several striking features as compared with those of the previously investigated systems involving ammonia borane. We found that the decomposition of the complex in toluene solutions and upon heating the solid gives the same intermediate, releasing 2 equiv of hydrogen at 70 °C. It occurs at a temperature considerably lower than that for the pure  $\text{NH}_3\text{BH}_3$ , desorbing the first equivalent at 120 °C and the second at 150 °C.<sup>69</sup> To the best of our knowledge, this is the first metal borohydride–ammonia borane complex, resulting in hydrogen release. The other systems produce significant amounts of ammonia, diborane, and borazine on the first decomposition step.<sup>46–49</sup> Also, we do not observe polyamino-boranes (PAB) and polyborazylene, which form during liquid-state pyrolysis of  $\text{NH}_3\text{BH}_3$  in ionic liquids and in the presence of strong Lewis and Brønsted acids. They would result in  $^{11}\text{B}$  signals in the range of  $-10$  to  $-13$  ppm for  $\text{BH}_2^+$ , near  $-5$  ppm for  $\text{N}-\text{BH}_2-\text{N}$ , and near  $-22$  ppm from  $\text{BH}_3$  polymer terminating groups for PAB and 26 ppm for polyborazylene.<sup>70,71</sup>

The favorable decomposition pathway and the decomposition temperature make this system an attractive model for efficient elimination of hydrogen from ammonia borane. Taking into account all our data, we conclude that the decomposition of the starting complex into the Al-based intermediate can be assigned to  $\text{Al}(\text{BH}_4)_3$  as a unique mild Lewis acid that coordinates both the starting and the dehydrogenated  $\text{BH}_n$  groups ( $n = 1$  or 3). This urges us to use other Al-based Lewis acids, less challenging with respect to stability and safety than aluminum borohydride.

This system is also encouraging in terms of a possible direct rehydrogenation of ammonia borane, which is currently regenerated successfully only via multistep chemical cycles.<sup>72</sup> The striking property of the title system is the endothermic dehydrogenation on the first decomposition step (39 kJ/mol, including melting), compared to the exothermic one for ammonia borane ( $-22$  kJ/mol on the first decomposition step, including melting).<sup>36</sup> Despite our first attempts to directly rehydrogenate the intermediate that were not successful, a catalyzed reaction may be possible.

## ■ ASSOCIATED CONTENT

## ■ Supporting Information

Supplementary XRD data with Rietveld refinements, NMR spectroscopy and volumetric data, and CIF files. This material is available free of charge via the Internet at <http://pubs.acs.org>.

## ■ AUTHOR INFORMATION

## Corresponding Author

\*Fax: +32 10 47 27 07. E-mail: [yaroslav.filinchuk@uclouvain.be](mailto:yaroslav.filinchuk@uclouvain.be).

## Notes

The authors declare no competing financial interest.

## ■ ACKNOWLEDGMENTS

This work was supported by the Académie Universitaire Louvain (AUL), Belgium, under Grant ADi/DB/1058.2011 and FNRS (CC 1.5169.12, PDR T.0169.13, EQP U.N038.13). We thank ESRF for the beam time allocation at the SNBL and D. Chenyshov and V. Dyadkin for support. We thank Prof. Michel Luhmer (ULB) for the deconvolution analysis of the  $^{27}\text{Al}$  NMR spectrum and Lars H. Jepsen and Prof. Torben R. Jensen (Aarhus University, Aarhus, Denmark) for help with MS analysis.

## ■ REFERENCES

- (1) Orimo, S.; Nakamori, Y.; Eliseo, J. R.; Züttel, A.; Jensen, C. M. *Chem. Rev.* **2007**, *107*, 4111–4132.
- (2) Ley, M. B.; Jepsen, L. H.; Lee, Y.-S.; Cho, Y. W.; Colbe, J. B.; Dornheim, M.; Rokhi, M.; Jensen, J. O.; Sloth, M.; Filinchuk, Y.; Jørgensen, J. E.; Besenbacher, F.; Jensen, T. R. *Mater. Today* **2014**, *17*, 122–128.
- (3) Chua, Y. S.; Chen, P.; Wu, G.; Xiong, Z. *Chem. Commun.* **2011**, *47*, 5116–5129.
- (4) Jepsen, L. H.; Ley, M. B.; Lee, Y.-S.; Cho, Y. W.; Dornheim, M.; Jensen, J. O.; Filinchuk, Y.; Jørgensen, J. E.; Besenbacher, F.; Jensen, T. R. *Mater. Today* **2014**, *17*, 129–135.
- (5) Klebanoff, L. E.; Keller, J. O. *Int. J. Hydrogen Energy* **2013**, *38*, 4533–4576.
- (6) Li, H.-W.; Yan, Y.; Oriomo, S.-I.; Züttel, A.; Jensen, C. M. *Energies* **2011**, *4*, 185–214.
- (7) Mao, J.; Guo, Z.; Nevikovets, I. P.; Liu, H. K.; Dou, S. H. *J. Phys. Chem. C* **2012**, *116*, 1596–1604.
- (8) Burg, A. B.; Schlesinger, H. I. *J. Am. Chem. Soc.* **1940**, *62*, 3425–3429.
- (9) Chlopek, K.; Frommen, C.; Lèon, A.; Zabara, O.; Fichtner, M. *J. Mater. Chem.* **2007**, *17*, 3496–3503.
- (10) Kim, Y.; Hwang, S.-J.; Shim, J.-H.; Lee, Y.-S.; Han, H. N.; Cho, Y. W. *J. Phys. Chem. C* **2012**, *116*, 4330–4334.
- (11) Schlesinger, H. I.; Sanderson, R. T.; Burg, A. B. *J. Am. Chem. Soc.* **1940**, *62*, 3421–3425.
- (12) Volkov, V. V.; Myakishev, K. G. *Izv. Sib. Otd. Akad. Nauk SSSR, Ser. Khim. Nauk* **1977**, *1*, 77–82.
- (13) Grochala, W.; Edwards, P. P. *Chem. Rev.* **2004**, *104*, 1283–1315.
- (14) Nakamori, Y.; Miwa, K.; Ninomiya, A.; Li, H.; Ohba, N.; Towata, S.; Züttel, A.; Orimo, S. *Phys. Rev. B* **2006**, *74*, 45126.
- (15) Rude, L. H.; Nielsen, T. K.; Ravnsbæk, D. B.; Bösenberg, U. M.; Ley, B.; Richter, B.; Arnbjerg, L. M.; Dornheim, M.; Filinchuk, Y.; Besenbacher, F.; Jensen, T. R. *Phys. Status Solidi A* **2011**, *208*, 1754–1773.
- (16) Lindemann, I.; Ferrer, R. D.; Dunsch, L.; Filinchuk, Y.; Černý, R.; Hagemann, H.; D'Anna, V.; Daku, L. M. L.; Schultz, L.; Gutfleisch, O. *Chem.—Eur. J.* **2010**, *16*, 8707–8712.
- (17) Lindemann, I.; Ferrer, R. D.; Dunsch, L.; Černý, R.; Hagemann, H.; D'Anna, V.; Filinchuk, Y.; Schultz, L.; Gutfleisch, O. *Faraday Discuss.* **2011**, *151*, 231–242.
- (18) Dovgaliuk, I.; Ban, V.; Sadikin, Y.; Černý, R.; Aranda, L.; Casati, N.; Devillers, M.; Filinchuk, Y. *J. Phys. Chem. C* **2014**, *118*, 145–153.
- (19) Ravnsbæk, D. B.; Filinchuk, Y.; Cerenius, Y.; Jakobsen, H. J.; Besenbacher, F.; Skibsted, J.; Jensen, T. R. *Angew. Chem., Int. Ed.* **2009**, *48*, 6659–6663.
- (20) Černý, R.; Ravnsbæk, D. B.; Schounwink, P.; Filinchuk, Y.; Penin, N.; Teyssier, J.; Smrčok, L.; Jensen, T. R. *J. Phys. Chem. C* **2012**, *116*, 1563–1571.
- (21) Ravnsbæk, D. B.; Sørensen, L. H.; Filinchuk, Y.; Besenbacher, F.; Jensen, T. R. *Angew. Chem., Int. Ed.* **2012**, *51*, 3582–3586.
- (22) Guo, Y. H.; Xia, G.; Zhu, Y.; Gao, L.; Yu, X. *Chem. Commun.* **2010**, *46*, 2599–2506.
- (23) Guo, Y. H.; Sun, W. W.; Guo, Z. P.; Liu, H. K.; Sun, D. L.; Yu, X. B. *J. Phys. Chem. C* **2010**, *114*, 12823–12827.
- (24) Soloveichik, G.; Her, J.-H.; Stephens, P. W.; Gao, Y.; Rijssenbeek, J.; Andrus, M.; Zhao, J.-C. *Inorg. Chem.* **2008**, *47*, 4290–4298.
- (25) Chu, H.; Wu, G.; Xiong, Z.; Guo, J.; He, T.; Chen, P. *Chem. Mater.* **2010**, *22*, 6021–6028.
- (26) Gu, Q.; Gao, L.; Guo, Y.; Tan, Y.; Wallwork, K. S.; Zhang, F.; Yu, X. *Energy Environ. Sci.* **2012**, *5*, 7590–7600.
- (27) Yuan, F.; Gu, Q.; Chen, X.; Tan, Y.; Guo, Y.; Yu, X. *J. Mater. Chem.* **2012**, *24*, 3370–3379.
- (28) Guo, Y. H.; Yu, X.; Sun, W.; Sun, D.; Yang, W. *Angew. Chem., Int. Ed.* **2011**, *50*, 1087–1091.
- (29) Guo, Y. H.; Jiang, Y.; Xia, G.; Yu, X. *Chem. Commun.* **2012**, *48*, 4408–4410.
- (30) Sun, W.; Chen, X.; Gu, Q.; Wallwork, K. S.; Tan, Y.; Tang, Z.; Yu, X. *Chem.—Eur. J.* **2012**, *18*, 6825–6834.
- (31) Yang, Y.; Liu, Y.; Wu, H.; Zhou, W.; Gao, M.; Pan, H. *Phys. Chem. Chem. Phys.* **2014**, *16*, 135–143.
- (32) Guo, Y.; Wu, H.; Zhou, W.; Yu, X. *J. Am. Chem. Soc.* **2011**, *133*, 4690–4693.
- (33) Johnson, S. R.; David, W. I. F.; Royse, D. M.; Sommariva, M.; Tang, C. Y. F.; Fabbiani, P. A.; Jones, M. O.; Edwards, P. P. *Chem.—Asian J.* **2009**, *4*, 849–854.
- (34) Zheng, X.; Wu, G.; Li, W.; Xiong, Z.; He, T.; Guo, J.; Chen, H.; Chen, P. *Energy Environ. Sci.* **2011**, *4*, 3593–3600.
- (35) Chen, X.; Yu, X. *J. Phys. Chem. C* **2012**, *116*, 11900–11906.
- (36) Wolf, G.; Baumann, J.; Baitalow, F.; Hoffmann, F. P. *Thermochim. Acta* **2000**, *343*, 19–25.
- (37) Baitalow, F.; Baumann, J.; Wolf, G.; Jaenicke-Röbber, K.; Leiter, G. *Thermochim. Acta* **2002**, *391*, 159–168.
- (38) Xiong, Z.; Yong, C. K.; Wu, G.; Chen, P.; Shaw, W.; Karkamkar, A.; Autrey, T.; Jones, M. O.; Johnson, S. I.; Edwards, P. P.; David, W. I. F. *Nat. Mater.* **2008**, *7*, 138–141.
- (39) Diyabalanage, H. V. K.; Shrestha, R. P.; Semelsberger, T. A.; Scott, B. L.; Bowden, M. E.; Davis, B. L.; Burelli, A. K. *Angew. Chem., Int. Ed.* **2007**, *46*, 8995–8997.
- (40) Wu, H.; Zhou, W.; Yildirim, T. *J. Am. Chem. Soc.* **2008**, *130*, 14834–14839.
- (41) Luo, J.; Kang, X.; Wang, P. *Energy Environ. Sci.* **2013**, *6*, 1018–1025.
- (42) Fijalkowski, K. J.; Genova, R. V.; Filinchuk, Y.; Budzianowski, A.; Derzci, M.; Jaroń, T.; Leszczynski, P. J.; Grohala, W. *Dalton Trans.* **2011**, *40*, 4407–4413.
- (43) Wu, H.; Zhou, W.; Pinkerton, F. E.; Meyer, M. S.; Yao, Q.; Gadipelli, S.; Yildirim, T.; Rush, J. J. *Chem. Commun.* **2011**, *47*, 4102–4204.
- (44) Luo, J.; Wu, H.; Zhou, W.; Kang, X.; Fang, Z.; Wang, P. *Int. J. Hydrogen Energy* **2013**, *38*, 197–204.
- (45) Wu, C.; Wu, G.; Xiong, Z.; Han, X.; Chu, H.; He, T.; Chen, P. *Chem. Mater.* **2010**, *22*, 3–5.
- (46) Luo, J.; Wu, H.; Zhou, W.; Kang, X.; Fang, Z.; Wang, P. *Int. J. Hydrogen Energy* **2012**, *37*, 10750–10757.
- (47) Wu, H.; Zhou, W.; Pinkerton, F. E.; Meyer, M. S.; Srinivas, G.; Yildirim, T.; Udovic, T. J.; Rush, J. J. *J. Mater. Chem.* **2010**, *20*, 6550–6556.

- (48) Chen, X.; Yuan, F.; Gu, Q.; Yu, X. *Dalton Trans.* **2013**, *42*, 14365–14368.
- (49) Jepsen, L. H.; Ban, V.; Møller, K. T.; Lee, Y.-S.; Cho, Y. W.; Besenbacher, F.; Filinchuk, Y.; Skibsted, J.; Jensen, T. R. *J. Phys. Chem. C* **2014**, *118*, 12141–12153.
- (50) Tan, Y.; Gu, Q.; Kimpton, J. A.; Li, Q.; Chen, X.; Ouyang, L.; Zhu, M.; Sun, D.; Yu, X. *J. Mater. Chem. A* **2013**, *1*, 10155–10165.
- (51) Schlesinger, H. I.; Brown, H. C.; Hyde, E. K. *J. Am. Chem. Soc.* **1953**, *75*, 209–213.
- (52) *Xcalibur/SuperNova CCD system, CrysAlisPro Software system*, version 1.171.36.24; Agilent Technologies UK Ltd.: Oxford, U.K., 2012.
- (53) Sheldrick, G. M. *Acta Crystallogr.* **2008**, *A64*, 112–122.
- (54) Hammersley, A. P.; Svensson, S. O.; Hanfland, M.; Fitch, A. N.; Häusermann, D. *High Pressure Res.* **1996**, *14*, 2358.
- (55) Rodríguez-Caryajal, J. *Physica B* **1993**, *192*, 55–69.
- (56) Filinchuk, Y.; Cerný, R.; Hagemann, H. *Chem. Mater.* **2009**, *21*, 925–933.
- (57) Filinchuk, Y.; Richter, B.; Jensen, T. R.; Dmitriev, V.; Chernyshov, D.; Hagemann, H. *Angew. Chem., Int. Ed.* **2011**, *50*, 11162–11166.
- (58) Almenningen, A.; Gundersen, G.; Haaland, A. *Acta Chem. Scand.* **1968**, *22*, 328–334.
- (59) Aldridge, S.; Blake, A. J.; Downs, A. J.; Gould, R. O.; Parsons, S.; Pullham, C. R. *J. Chem. Soc., Dalton Trans.* **1997**, 1007–1012.
- (60) Dou, D.; Liu, J.; Bauer, J. A. K.; Jordan, G. T., IV; Shore, S. G. *Inorg. Chem.* **1994**, *33*, 5443–5447.
- (61) Coe, D. A.; Nibler, J. W. *Spectrochim. Acta, Part A* **1973**, *29*, 1789–1804.
- (62) Jensen, J. O. *Spectrochim. Acta, Part A* **2003**, *59*, 1575–1578.
- (63) Hess, N. J.; Bowden, M. E.; Parvanov, V. M.; Mundy, C.; Kathmann, S. M.; Schender, G. K.; Autrey, T. *J. Chem. Phys.* **2008**, *128*, 34508.
- (64) Downs, A. J.; Jones, L. A. *Polyhedron* **1994**, *13*, 2401–2415.
- (65) Chen, X.; Zhang, Y.; Wang, Y.; Zhou, W.; Knight, D. A.; Yisgedu, T. B.; Huang, Z.; Lingam, H. K.; Billet, B.; Udovic, T. J.; Brown, G. M.; Shore, S. G.; Wolverton, C.; Zhao, J.-C. *Chem. Sci.* **2012**, *3*, 3183–3191.
- (66) Lingam, H. K.; Chen, X.; Zhao, J.-C.; Shore, S. G. *Chem.—Eur. J.* **2012**, *18*, 3490–3492.
- (67) Maybury, P. C.; Ahnell, J. E. *Inorg. Chem.* **1967**, *6*, 1286–1291.
- (68) Nöth, H.; Rurländer, R. *Inorg. Chem.* **1981**, *20*, 1062–1072.
- (69) Karkamkar, A.; Aardahl, C.; Autrey, T. *Mater. Matters (Milwaukee, WI, U.S.)* **2007**, *2*, 6–9.
- (70) (a) Bluhm, M. E.; Bradley, M. G.; Butterick, R., III; Kusari, U.; Sneddon, L. G. *J. Am. Chem. Soc.* **2006**, *128*, 7748–7749. (b) Himmelberger, D. W.; Alden, L. R.; Bluhm, M. E.; Sneddon, L. G. *Inorg. Chem.* **2009**, *48*, 9883–9889.
- (71) Stephens, F. H.; Baker, R. T.; Matus, M. H.; Grant, D. J.; Dixon, D. A. *Angew. Chem., Int. Ed.* **2007**, *46*, 746–749.
- (72) (a) Sutton, A. D.; Burrell, A. K.; Dixon, D. A.; Garner, E. B., III; Gordon, J. C.; Nakagawa, T.; Ott, K. C.; Robinson, J. P.; Vasiliu, M. *Science* **2011**, *331*, 1426–1429. (b) Summerscales, O. T.; Gordon, J. C. *Dalton Trans.* **2013**, *42*, 10075–10084.